Electronic Supplementary Material (ESI) for Journal of Materials Chemistry B.
This journal is © The Royal Society of Chemistry 2023

Supplementary Material

Spherical Porous Iron-Nitrogen-Carbon Nanozyme Derived from Tannin Coordination Framework for Preparation of L-DOPA by Emulating Tyrosine Hydroxylase

Chan Chen[#], Haisheng Ren[#], Weikang Tang, Mengqi Han, Qinfei Chen, Hong Zhou, Jiadong Chen, Yuyue Gao, Wenbin Liu*

Department of Pharmaceutical and Biological Engineering, School of Chemical Engineering, Sichuan University, Chengdu 610065, China.

[#] These authors contributed equally: Chan Chen, Haisheng Ren.

* Corresponding author. Email address: wbliu@scu.edu.cn

ORCID ID: 0000-0002-3780-9394

Table of contents

1. Methods

1.1 Parameter definition

Yield was calculated as the percent for moles of DOPA produced per initial moles of Tyr used. Conversion was defined as the percentage of moles of Tyr reacted/moles of initial Tyr used. Selectivity was defined as the mole percentage of DOPA formed per starting moles of Tyr converted. Productivity was defined as the amount of DOPA produced per hour. They were calculated according to the following definitions and equations.

$$Yield\ (\%) = \frac{C_D}{C_{T_0}} \times 100\% \qquad \#(1)$$

$$Conversion\ (\%) = \left(1 - \frac{C_T}{C_{T_0}}\right) \times 100\% \qquad \#(2)$$

$$Selectivity\ (\%) = \frac{Yield\ (\%)}{Conversion\ (\%)} \times 100\% \qquad \#(3)$$

$$Productivity\ \left(mg{\cdot}L^{-1}{\cdot}\ h^{-1}\right) = \frac{C_D \times 60 \times 197.16}{T} \qquad \#(4)$$

where C_D means the concentration of DOPA after reaction, mM; C_{T_0} means the initial concentration of Tyr, mM; C_T means the concentration of Tyr after reaction, mM; T means the time of reaction, min.

1.2 Determination of catalytic kinetic parameters

Michaelis-Menten constant K_m and maximal reaction velocity υ_{max} were calculated using the Michaelis-Menten equation (5):

$$v = \frac{v_{max} \times\ [S]}{K_m + [S]} \qquad \#(5)$$

where υ is the initial velocity, and [S] is the substrate concentration. Rate constant k_{cat} was calculated according to literatures[1, 2] using equation (6):

$$k_{cat} = \frac{v_{max}}{[E]} \qquad \#(6)$$

where $[E]$ is the molar concentration of nanozyme as calculated by equation (7):

$$[E] = \frac{\rho_e}{m_s \times N_A} \qquad \#(7)$$

where ρ_e is the mass concentration of nanozyme in unit of g L^{-1}, m_s is the mass of a single nanozyme particle in unit of g, and N_A is Avogadro's constant (6.02×10^{23} mol^{-1}). m_s was calculated using equation (8):

$$m_s = \frac{\rho_s \times \pi \times d^3 \times 10^{-21}}{6} \qquad \#(8)$$

where ρ_s is the density of nanozyme in unit of g cm^{-3}, d is the average diameter of a nanozyme particle (nm) measured by SEM. To measure the density of nanozyme, 100 mg nanozyme was compressed as a tablet of 10 mm diameter and 0.48 mm height under 14 MPa for 1 min. Subsequently, the mass of tablet was measured. The volume of the tablet was calculated as 38.06 mm^3. The density of nanozyme was calculated.

1.3 XAS measurement

XAS measurements for Fe K-edge were obtained under ambient conditions at the beamline 07A1 Taiwan Light Source (TLS) of National Synchrotron Radiation Research Center, China. This beamline adopted fixed-exit double crystal Si (111) monochromator to ranging the X-ray energy from 5-23 KeV. The end-station equipped three ionization chambers and Lytle detector for transmission and fluorescence mode X-ray absorption spectroscopy with 7-element Silicon Drift Detector. The beam size of X-ray on the sample was about 0.5×0.25 mm (HxV) with flux higher than 1×10^{10} photon sec^{-1}. Samples were pelletized as disks of 13 mm diameter with 1mm thickness using graphite powder as a binder. The data were extracted and processed according to the standard procedures using ATHENA and ARTEMIS module implemented in the IFEFFIT software package.

Fe foil, FeO, Fe_2O_3, and iron phthalocyanine (FePc) were used as references.

For the XANES spectra, the experimental absorption coefficients as a function of energy μ(E) were processed by background subtraction and normalization procedures. For the EXAFS, the post-edge background was subtracted from the overall absorption and then normalized with respect to the edge-jump step. Fourier-transformed (FT) of k^2 weighting χ(k) in R space were analyzed by applying a hanning windows to separate the EXAFS contributions from different coordination shells. The four parameters, coordination number, bond length, Debye-Waller factor σ^2 and the inner potential correction ΔE_0 were fitted without anyone was fixed. To obtain the quantitative structural parameters around central atoms, least-squares curve parameter fitting was performed.

1.4 Electrochemical assay

Electrochemical studies were conducted using Chenhua CHI660E electrochemical workstation (Shanghai, China). A three-electrode reaction system was adopted with saturated calomel electrode as reference electrode, and graphite electrode as counter electrode, respectively. 5 mg catalyst powder were ultrasonically suspended in 980 μL ethanol solution containing 20 μL Nafion for 30 min. Working electrodes was prepared by spreading 5 μL the homogeneous as-prepared catalyst slurry onto a pre-polished glassy carbon electrode (d=3 mm) with mass loading of 0.28 mg cm^{-2} after drying in air. 20 mL 0.2 M glycine hydrochloride buffer (pH 4.5) was used as electrolyte. Scan rate was 50 mV s^{-1}.

1.5 DFT calculation

First-principle DFT calculations were implemented using Vienna ab initio Simulation Package (VASP). The generalized gradient approximation (GGA) of spin polarized Perdew-Burke-Ernzerholf (PBE) functionals was adopted to describe the exchange-correlation potential. The

projected augmented wave (PAW) method was used to describe the core electrons by periodic plane-wave basis with kinetic cutoff energy of 400 eV. The optimization and transition-state search were completed until the residual force converged to less than 0.04 eV $Å^{-1}$. Adsorption of H_2O_2 on material was simulated by a 5 × 5 supercell. The 3×3×1 Monkhorst-Pack *k*-point sampling was employed. A vacuum space of about 15 Å was added in the z direction for all the periodic slab models to avoid interactions between two adjacent images. Both the lattice constants and positions of all atoms were fully relaxed until the force was smaller than 0.04 eV/Å. The convergence energy threshold was set to 1×10^{-4} eV for self-consistent calculations.

The adsorption energy E_{ads} were calculated according using equation (9):

$$E_{ads} = E_{mol/surf.} - (E_{surf} + E_{mol}) \quad (9)$$

where E_{mol}, E_{surf}, and $E_{mol/surf.}$ denote the energy of the molecules, pure surface, and surface with the adsorbate, respectively.

2. Tables

Table S1. Sum of element contents

	Samples	Element contents (%)			
		C 1s	N 1s	O 1s	Fe 2p
XPS	TUFF-I-TE	95.08	1.59	2.98	0.35
	TUFF-I-T	93.41	1.87	4.54	0.17
	TUFF-I	63.63	6.16	29.15	1.05
	TUFF-TE	92.89	2.32	4.79	
ICP-OES/EA	TUFF-I-TE	91.63	0.58	4.28	3.51

Table S2. Binding energy and area ratio of species for samples in XPS spectra

Element	Components	TUFF-I-TE		TUFF-I-T		TUFF-I		TUFF-TE		TUFF-I-TE after usage	
		Binding energy (eV)	Area (%)	Binding energy (eV)	Area (%)	Binding energy (eV)	Area (%)	Binding energy (eV)	Area (%)	Binding energy (eV)	Area (%)
C	Graphitic C	284.8	40.6	284.8	40.7	284.8	99.1	284.8	35.6	284.8	51.4
	C=N	285.2	28.2	285.2	28.3	-	-	285.2	35.5	285.9	11.6
	Fe_3C	287.0	3.8	287.0	3.7	-	-	-	-	287.0	9.3
	C-N	288.7	27.5	288.7	27.3	288.7	0.9	288.7	28.9	288.7	27.8
N	Pyridinic-N	398.1	9.7	398.1	10.2	398.1	16.8	398.1	12.4	396.0	2.6
	Fe–Nx	398.9	8.6	398.9	12.0	398.9	40.7	-	-	398.0	4.9
	Pyrrolic-N	-	-	-	-	400.1	30.2	-	-	400.1	35.4
	Graphitic-N	401.3	47.7	401.3	57.1	401.3	12.4	401.3	71.5	401.3	36.9
	Oxidized-N	406.0	34.1	405.0	20.7	-	-	405.0	16.1	406.0	20.2
O	C-O-Fe	530.5	11.0	530.5	14.3	530.5	51.7	-	-	530.5	1.9
	C-C=O	531.4	24.2	531.4	21.8	531.4	31.9	531.4	18.3	532.2	14.4
	C-O-C	532.2	31.4	532.2	30.6	532.2	15.0	532.2	40.1	533.0	48.0
	O-C=O	533.6	33.4	533.6	33.3	533.6	1.5	533.6	41.6	533.6	35.7
Fe	Fe_3C	708.1	3.4	708.1	6.4	708.1	4.7	-	-	705.1	25.6
	$Fe^{2+}2p_{3/2}$	711.5	26.0	711.1	18.4	711.2	28.7	-	-	710.3	11.3
	$Fe^{3+}2p_{3/2}$	714.4	28.9	714.4	27.3	714.4	26.6	-	-	714.4	25.4
	$Fe^{2+}2p_{1/2}$	724.6	14.1	724.2	17.8	724.3	26.3	-	-	724.6	20.6
	$Fe^{3+}2p_{1/2}$	727.5	27.7	727.5	30.1	727.5	13.7	-	-	727.5	17.1

Table S3. EXAFS fitting parameters at the Fe K-edge

Sample	Shell	N	R (Å)	σ^2	ΔE_0	R factor
TUFF-I-TE	Fe-N	0.90±0.2	1.91±0.02	0.001	3.00±0.8	0.005
	Fe-Fe	12.21±0.4	2.55±0.01	0.014		

N: coordination numbers; R: bond distance; σ^2: Debye-Waller factors; ΔE_0: the inner potential correction. R factor: goodness of fit; passive electron factor S_0^2=0.74.

Table S4. Comparison of the kinetic constant of SPINC with those of natural enzymes and nanozymes

Catalyst	Enzyme mimic	Substrate	[E] (mM)	K_m (mM)	v_{max} (μM s^{-1})	k_{cat} (s^{-1})	k_{cat}/K_m ($mM^{-1}s^{-1}$)	Reference
Zn–N–C SAzyme	peroxidase	H_2O_2	2.15×10^{-11}	40.16	0.12	4.97×10^{6}	1.24×10^{5}	Ref[3]
Fe–N-rGO sheets	peroxidase	H_2O_2	1.20×10^{-8}	43.00	1.44	1.20×10^{5}	2.79×10^{3}	Ref[4]
Fe–N–C SAzyme	peroxidase	H_2O_2	1.60×10^{-8}	28.30	0.43	2.68×10^{4}	9.46×10^{2}	Ref[5]
Fe–N–C SAzyme	peroxidase	TMB	1.70×10^{-4}	0.13	0.16	0.92	7.09	Ref[6]
Fe–N–C SAzyme	peroxidase	TMB	1.48×10^{-3}	3.60	1.16	0.78	0.22	Ref[7]
Cu–N–C nanozyme	laccase	epinephrine	3.83×10^{-7}	0.58	0.46	0.12×10^{4}	0.21×10^{4}	Ref[1]
Horseradish peroxidase	/	H_2O_2	2.50×10^{-8}	3.70	0.09	3.50×10^{3}	9.46×10^{2}	Ref[8]
laccase	/	epinephrine	1.55×10^{-3}	0.16	0.05	0.03	0.21	Ref[1]
Tyrosine hydroxylase	/	tyrosine	/	0.02	/	2.50	0.15×10^{3}	Ref[9]
SPINC	tyrosine hydroxylase	tyrosine	6.64×10^{-9}	2.30	0.25	3.77×10^{4}	1.64×10^{4}	This study

Table S5. Reaction conditions for optimization steps

Conditions	Tyr (mM)	Catalyst (mg/ml)	ascorbic acid (mM)	H_2O_2(mM)	pH
A	1	0.4	1	2	4.5
B	1	0.2	1	2	4.5
C	1	0.2	1	5	4.5
D	1	0.2	4	5	4.5
E	5	0.2	4	5	4.5
F	5	0.2	8	4	4.5

3. Schemes

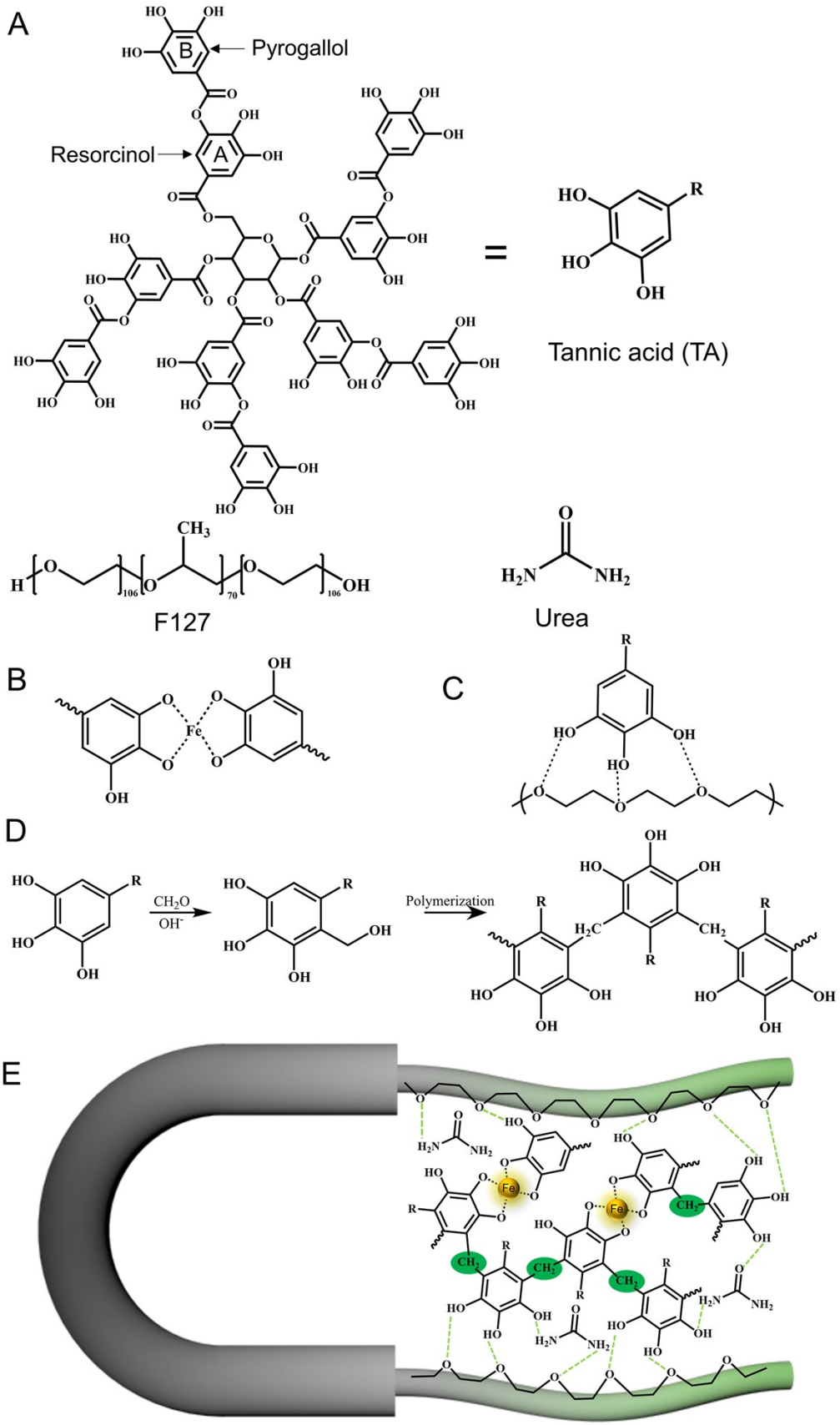
A
Pyrogallol
Resorcinol
Tannic acid (TA)
F127
Urea
B
C
D
Polymerization
E

Scheme S1. Interaction with tannic acid. (A) Chemical structure of precursors. (B) Coordination structure between tannic acid and iron ion. (C) Hydrogen bonding between tannic acid and F127. (D) Formation of oligomers via formaldehyde crosslinking. (E) Schematic illustration for tannin-iron coordination polymer.

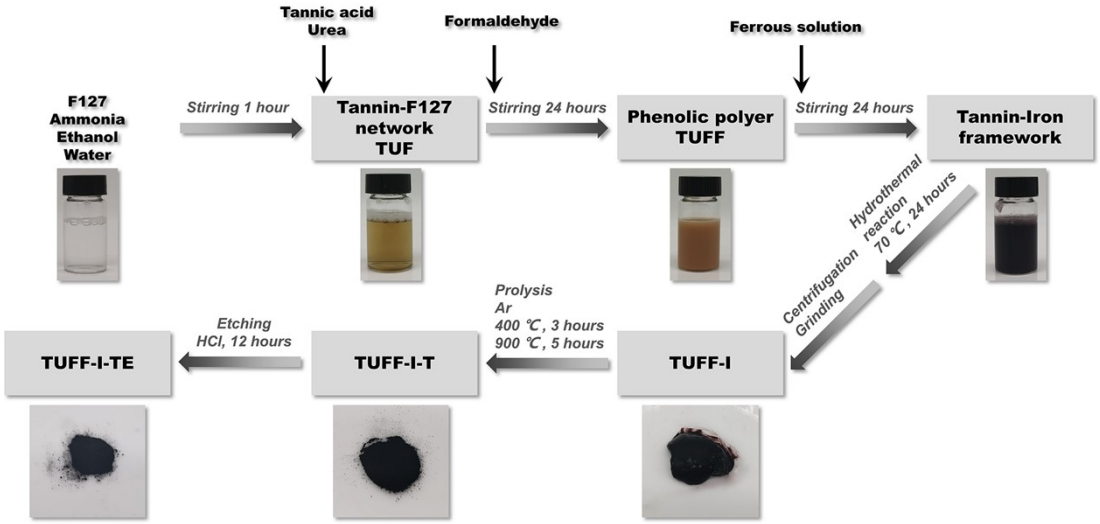

Scheme S2. Flow chart for synthesis route of SPINC nanozyme. Inset is corresponding photograph of samples for each step.

4. Figures

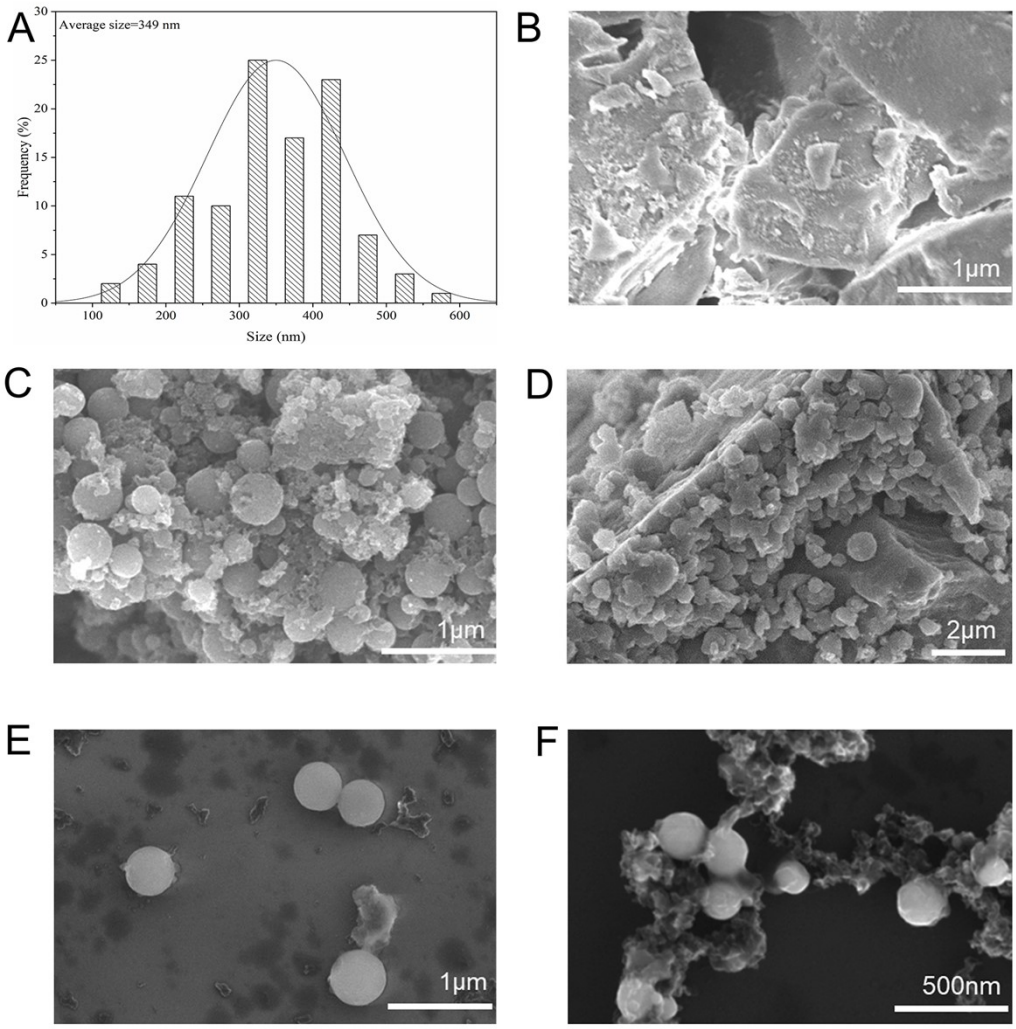

Figure S1. SEM of the material. (A) Histogram of diameter for TUFF-I-TE. (B) TUPF-I. (C) TUFF-TE. (D) TUFF-Z-TE. (E) TUFF-I. (F) TUFF-I-T.

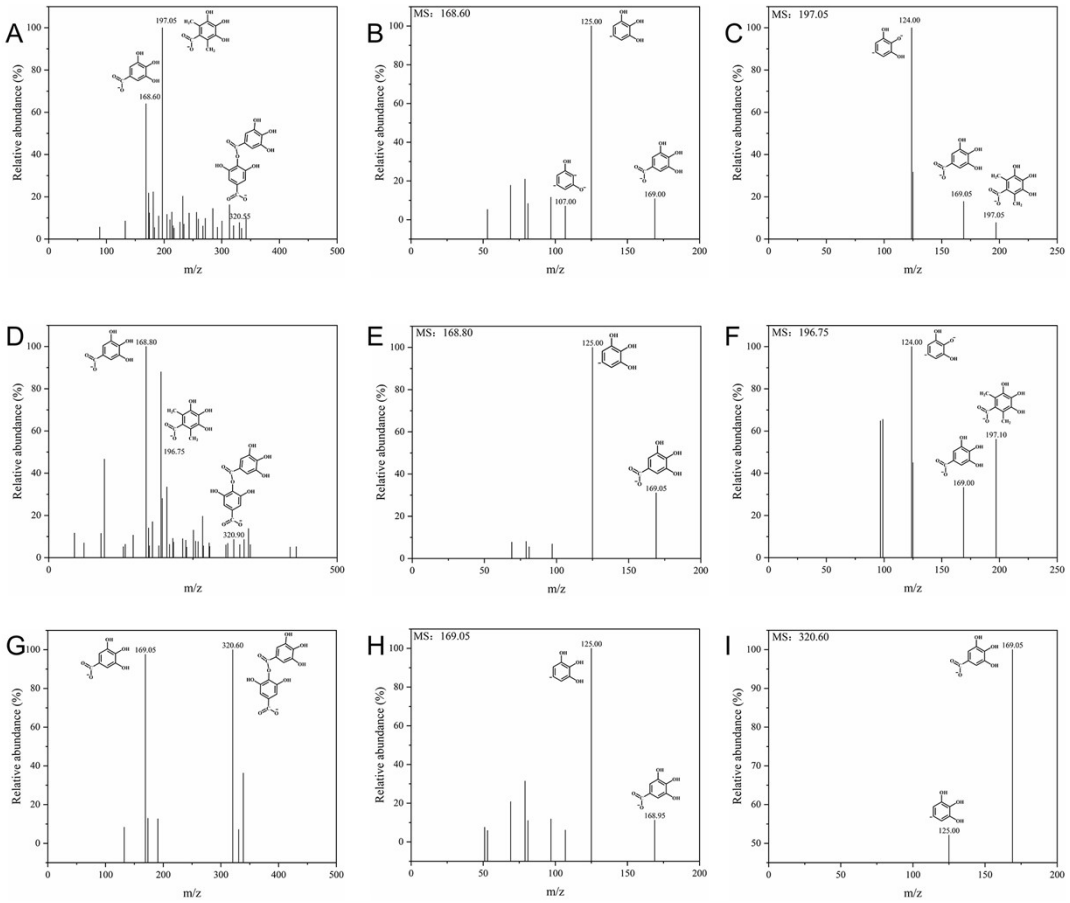

Figure S2. Mass spectrometry analysis for crosslinking of tannic acid. (A) MS profile of the phenolic polymer TUFF. (B) MS/MS for mother ion at m/z 168.60 in (A). (C) MS/MS for mother ion at m/z 196.05 in (A). (D) MS profile of reaction solution between tannic acid and formaldehyde in the presence of ethanol and ammonia. (E) MS/MS for mother ion at m/z 168.80 in (D). (F) MS/MS for mother ion at m/z 196.10 in (D). (G) MS profile of tannic acid. (H) MS/MS for mother ion at m/z 169.05 in (G). (I) MS/MS for mother ion at m/z 320.60 in (G).

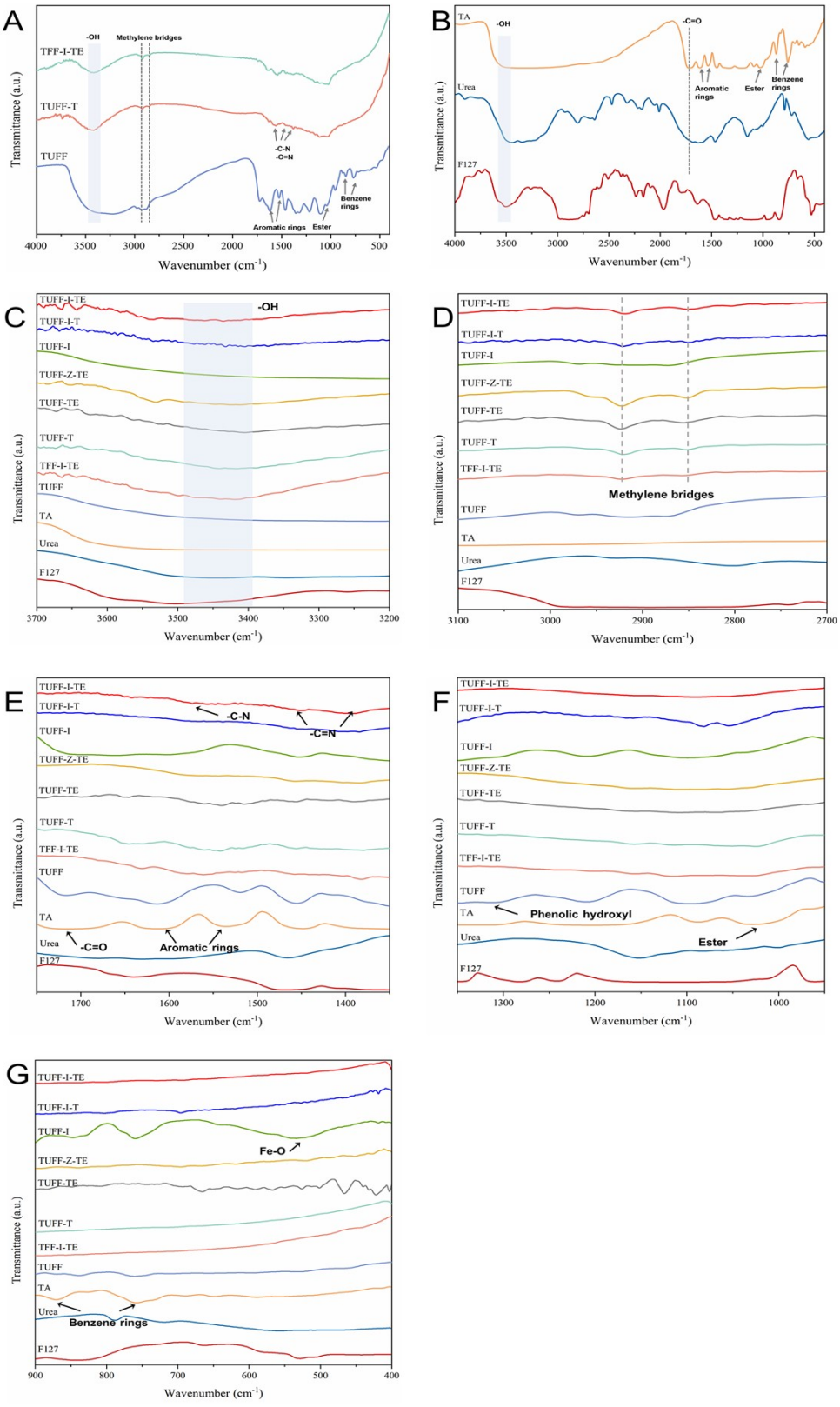

Figure S3. FTIR of control samples. (A) Nanomaterials. (B) Precursors. (C)-(G) Partial enlarged detail.

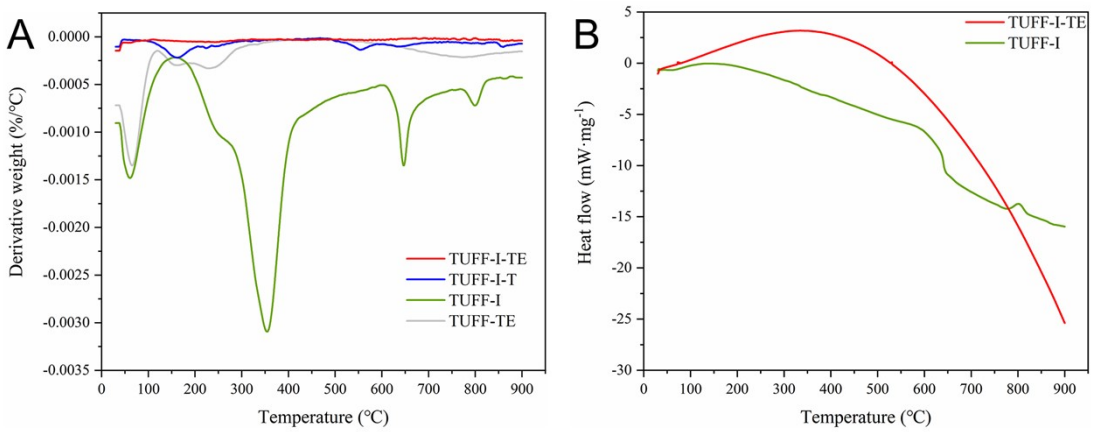

Figure S4. Thermogravimetry analysis. (A) DTG. (B) DSC patterns.

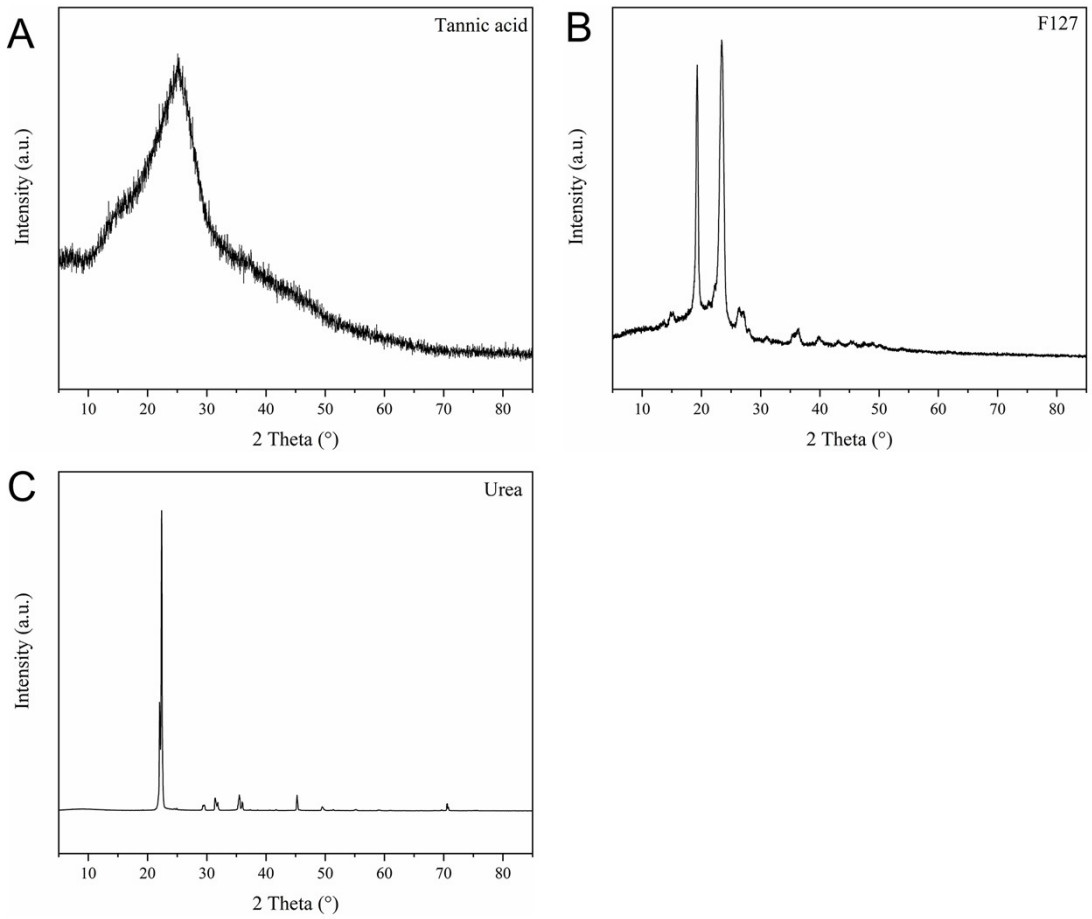

Figure S5. XRD of control samples. (A) Tannic acid. (B) F127. (C) Urea.

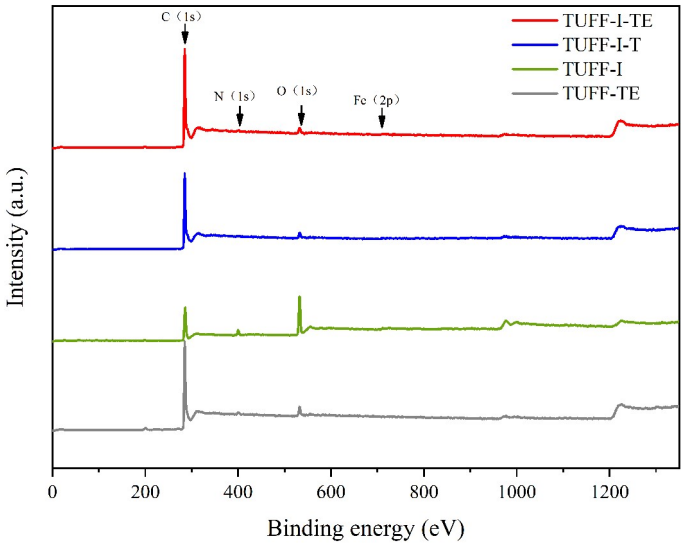

Figure S6. XPS survey spectrum.

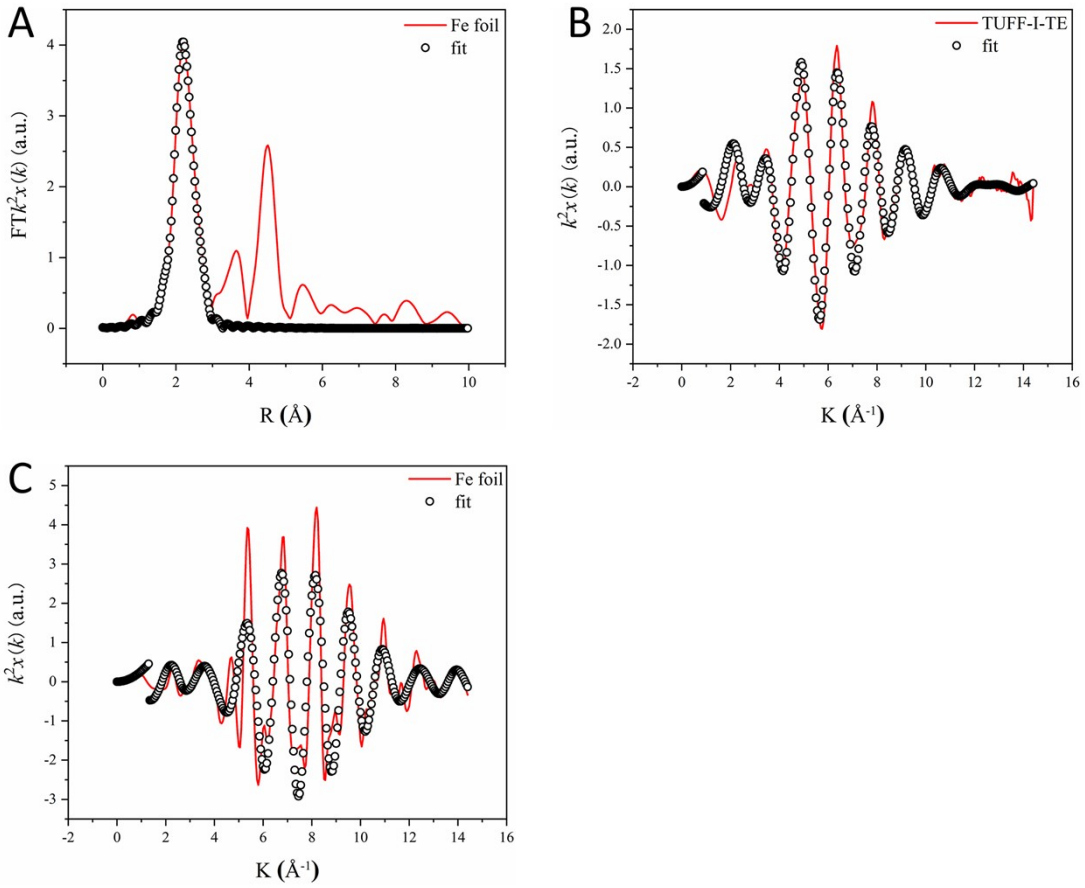

Figure S7. XAS spectra. (A) EXAFS fitting curves of TUFF-I-TE at *k* space. (B) EXAFS fitting curves of Fe foil at *R* space. (C) EXAFS fitting curves of Fe foil at *k* space.

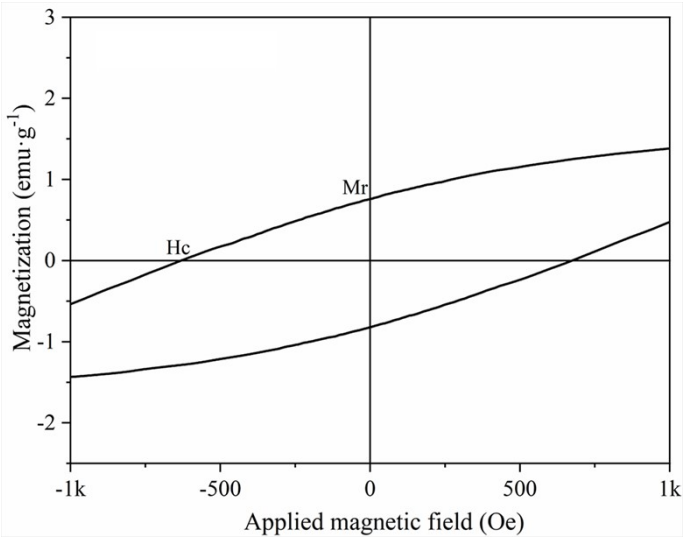

Figure S8. Enlarged image for magnetization curve.

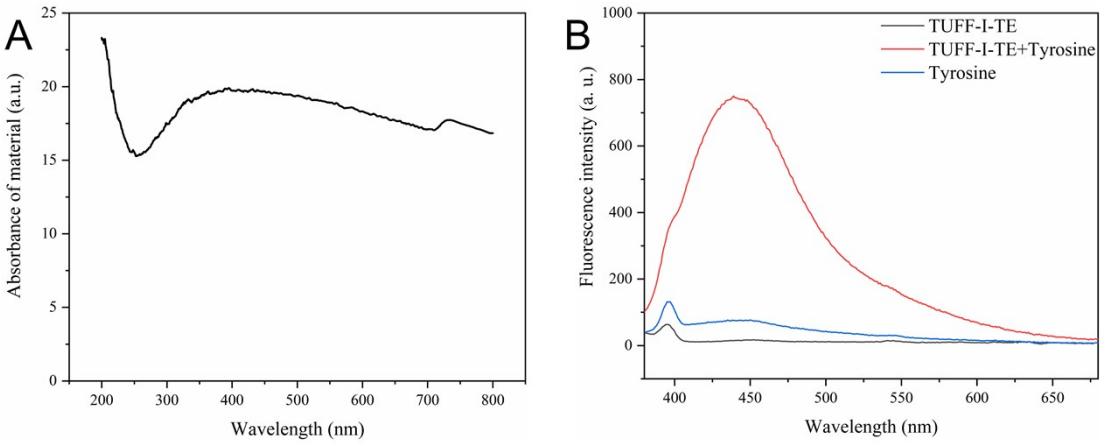

Figure S9. Optical property of TUFF-I-TE. (A) UV-visible diffuse reflectance spectra. (B) Fluorescence spectra. TUFF-I-TE, 0.4 mg mL^{-1}. [tyrosine]=1 mM. Ex= 350 nm.

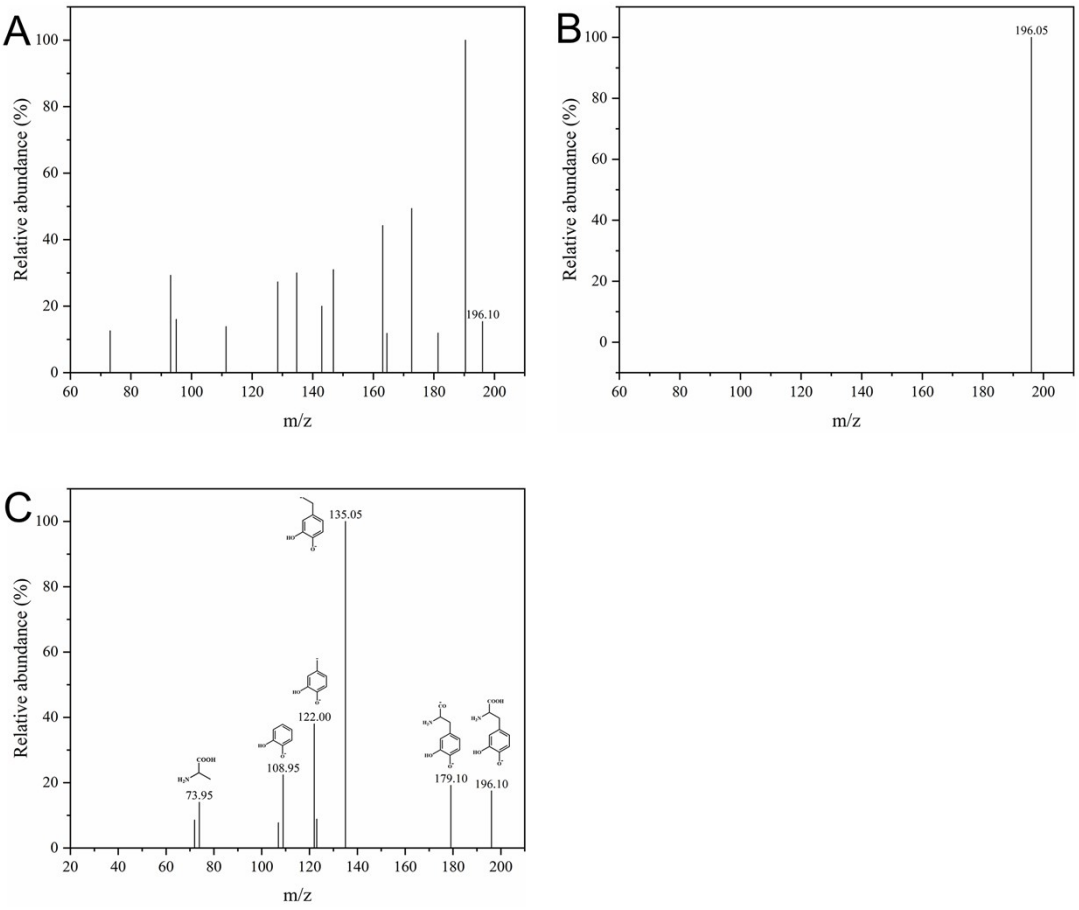

Figure S10. Identification of L-DOPA. (A) MS profile of reaction solution. (B) MS profile of L-DOPA standard. (C) MS/MS profile of L-DOPA standard.

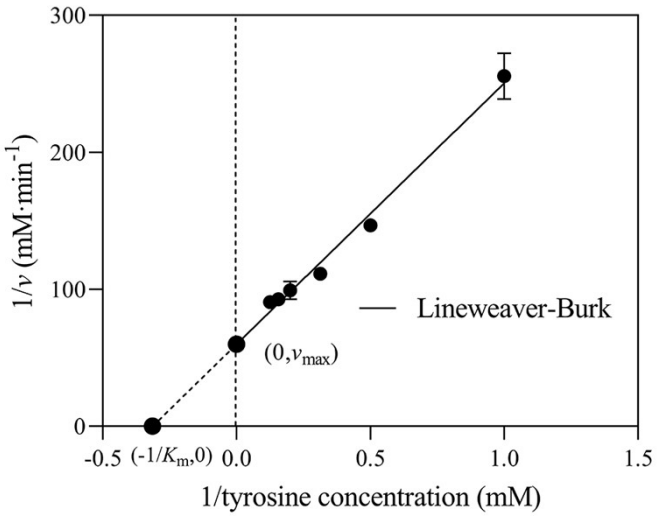

Figure S11. Lineweaver-Burk plot.

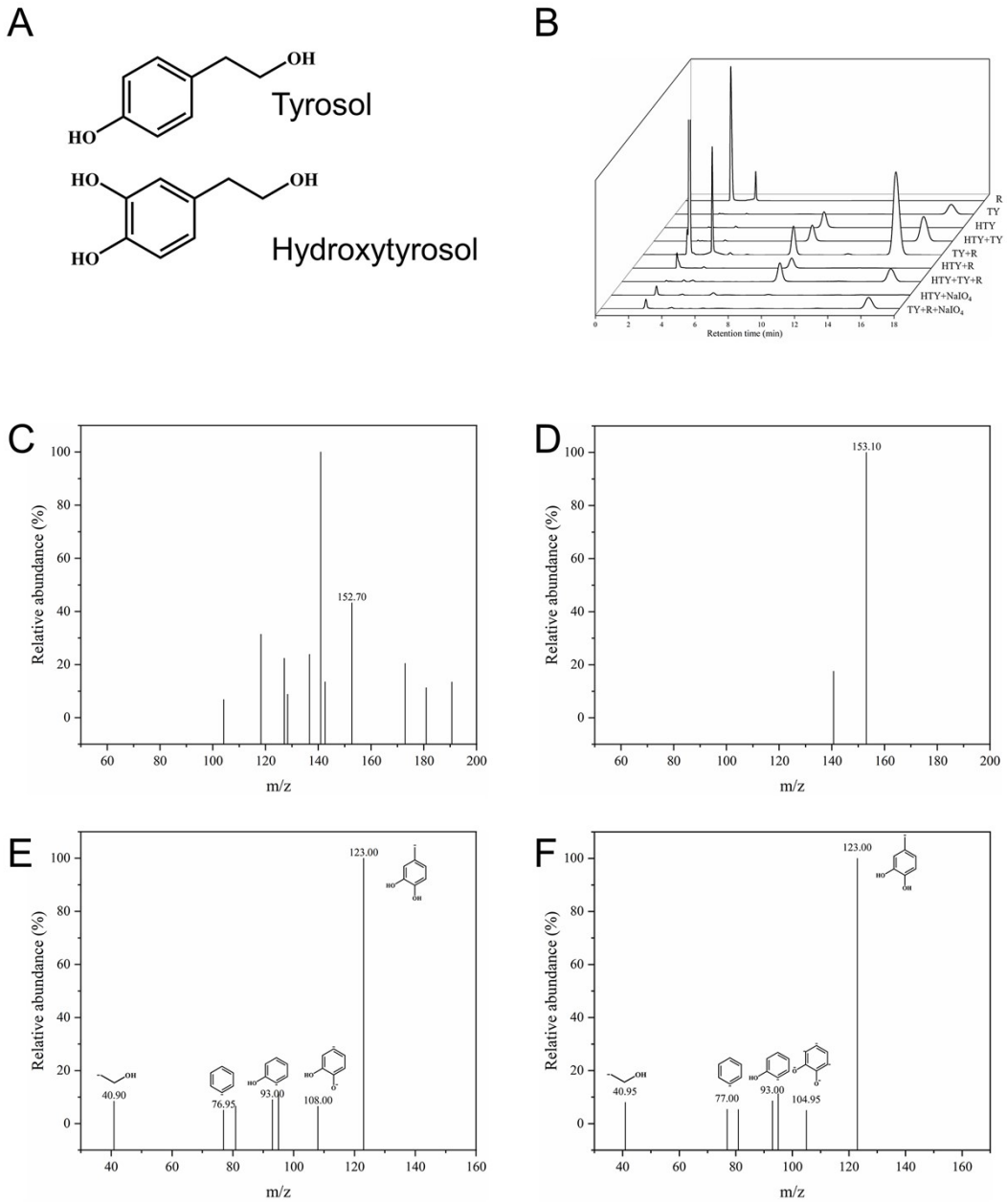

Figure S12. Catalysis for hydroxylation of tyrosol to hydroxytyrosol by SPINC nanozyme. (A) Chemical structure of tyrosol and hydroxytyrosol. (B) HPLC profile. TY, 10 mM tyrosol; HTY, 1 mM hydroxytyrosol; R, reaction mixture consisting of 0.4 mg mL^{-1} nanozyme, 10 mM ascorbic acid and 20 mM H_2O_2 in 0.2 M Gly-HCl buffer solution at pH 4.5. TY+R, tyrosol reacted with R at 25 °C for 60 minutes. TY+R+HTY, tyrosol reacted with R for 60 minutes and then was added with authentic hydroxytyrosol standard; $NaIO_4$: addition of 500 mM $NaIO_4$. (C) MS profile of reaction solution. (D) MS profile of hydroxytyrosol standard. (E) MS/MS profile of mother ion at m/z 152.70 in reaction solution. (F) MS/MS profile of hydroxytyrosol standard.

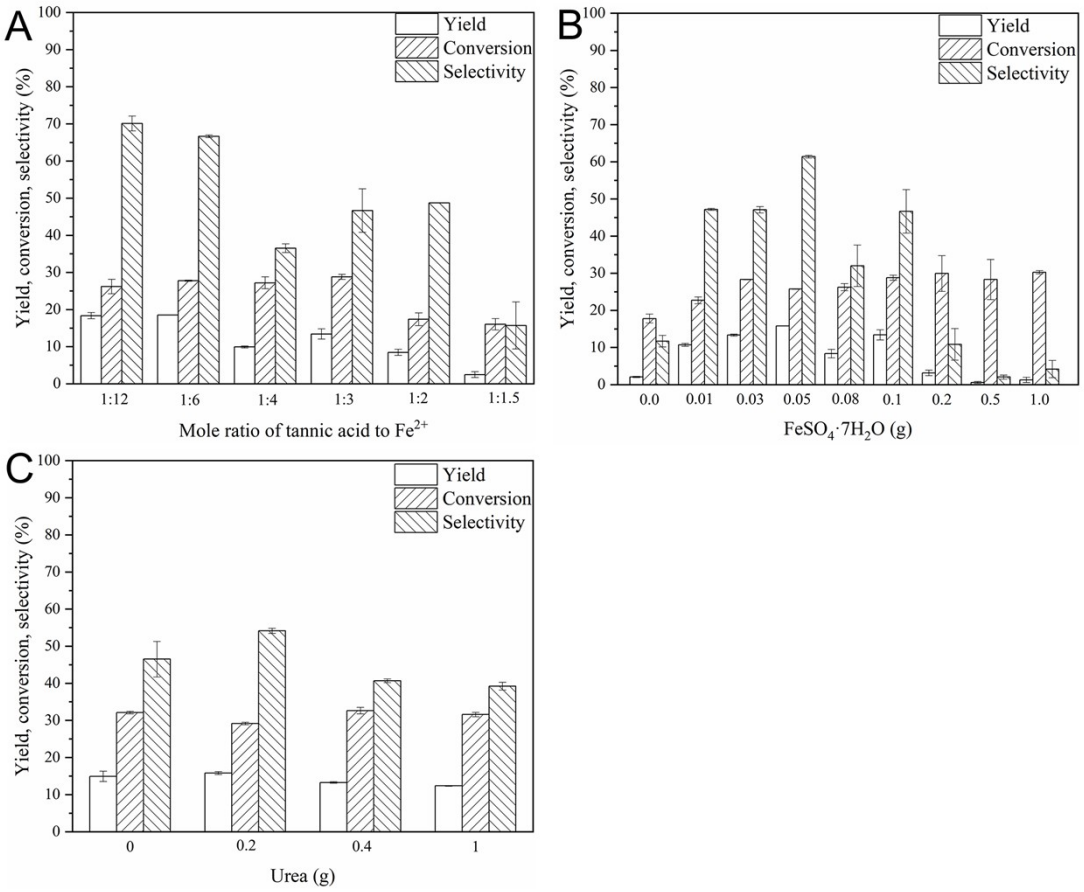

Figure S13. Effect of preparation condition on the catalytic activity of SPINC nanozyme. (A) Effect of mole ratio of tannic acid to Fe^{2+}. (B) Effect of iron ion dosage. (C) Effect of urea dosage.

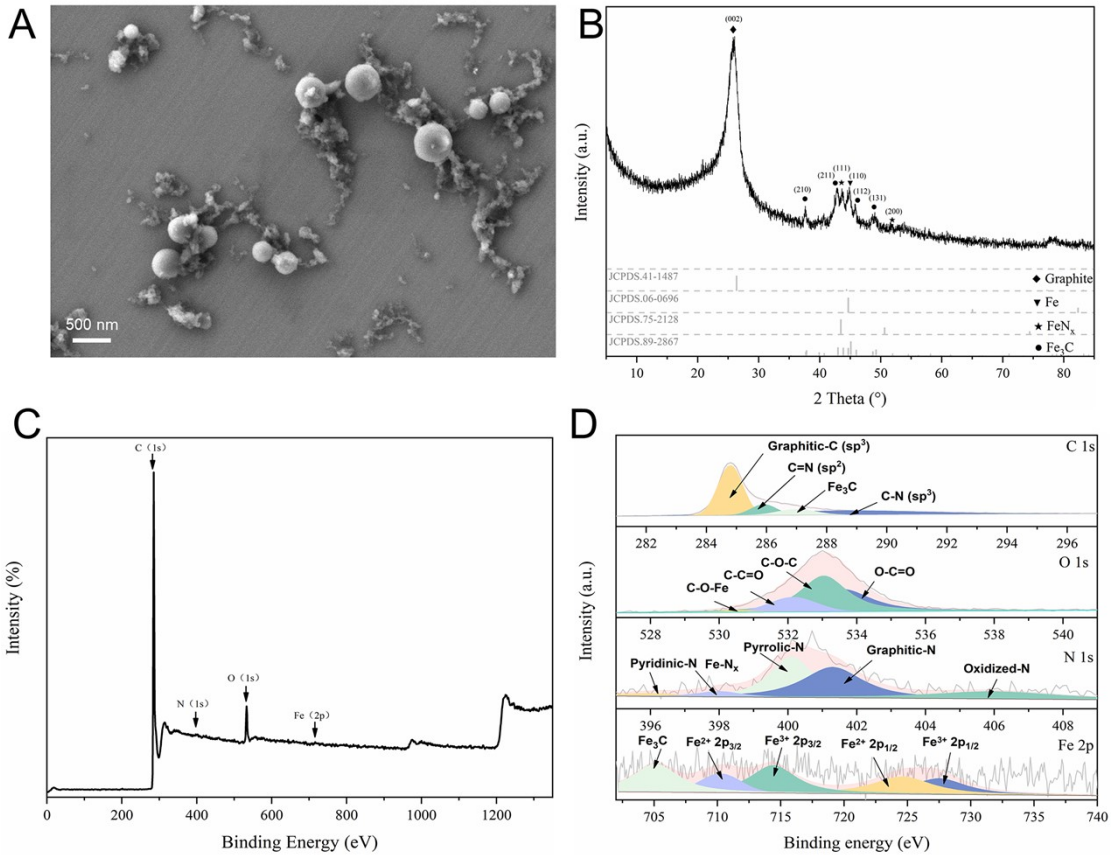

Figure S14. Characterization of SPINC nanozyme after usage. (A) SEM. (B) XRD. (C) XPS survey spectrum. (D) High-resolution XPS spectra.

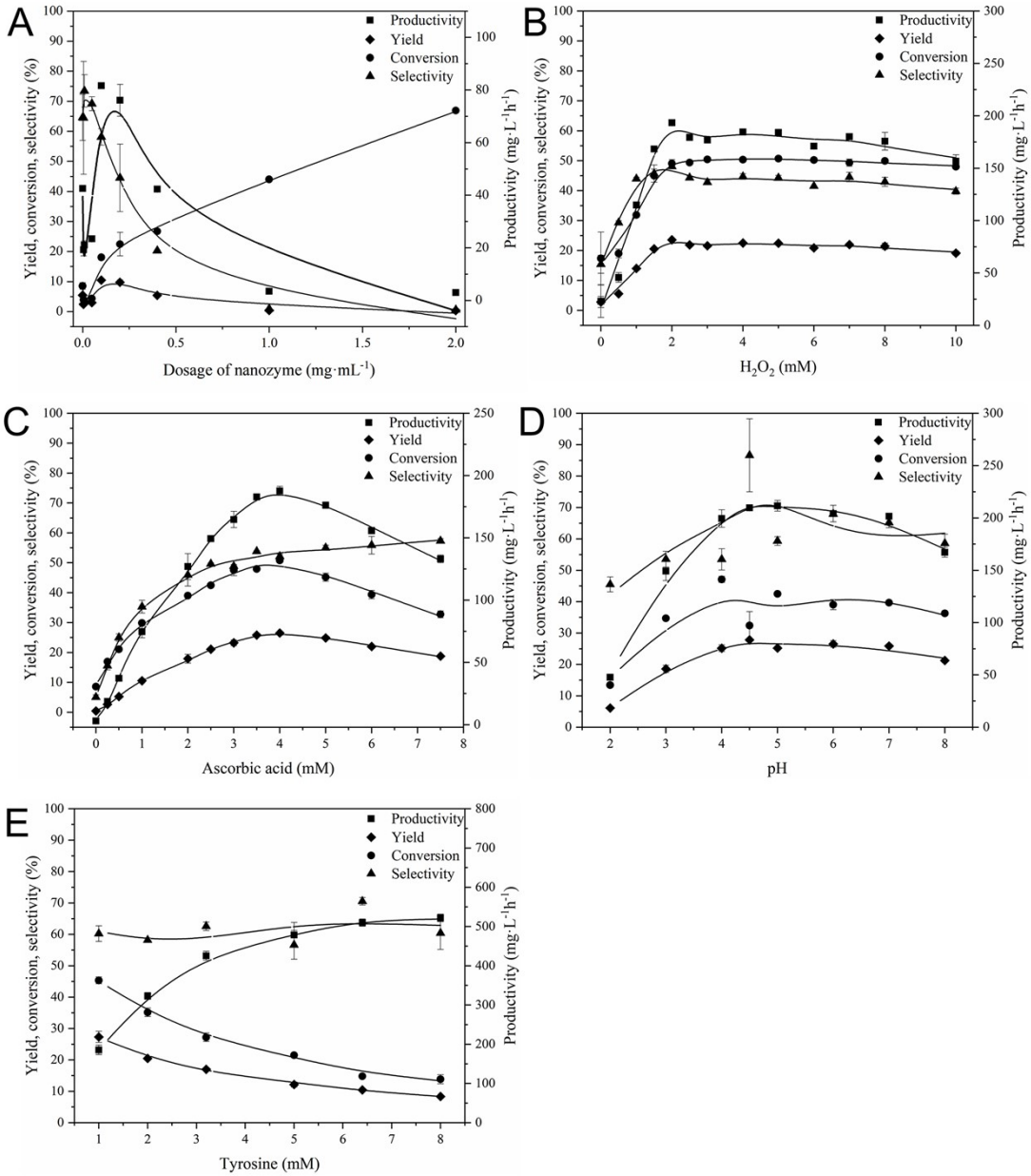

Figure S15. Optimization on reaction conditions for production of L-DOPA. [tyrosine] = 1 mM. (A) Effect of nanozyme dosage. (B) Effect of H_2O_2 concentration. (C) Effect of ascorbic acid concentration. (D) Effect of pH. (E) Effect of tyrosine concentration.

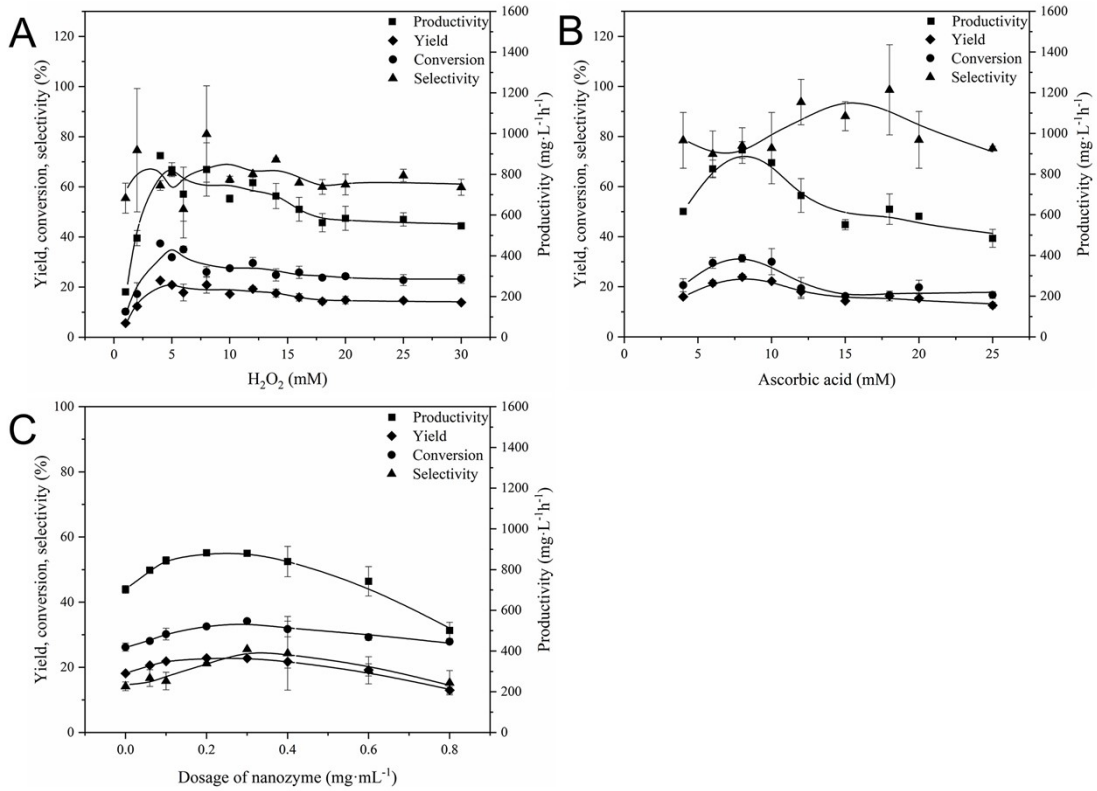

Figure S16. Optimization at high substrate concentration. [tyrosine] = 5 mM. (A) Effect of H_2O_2 concentration. (B) Effect of ascorbic acid concentration. (C) Effect of nanozyme dosage.

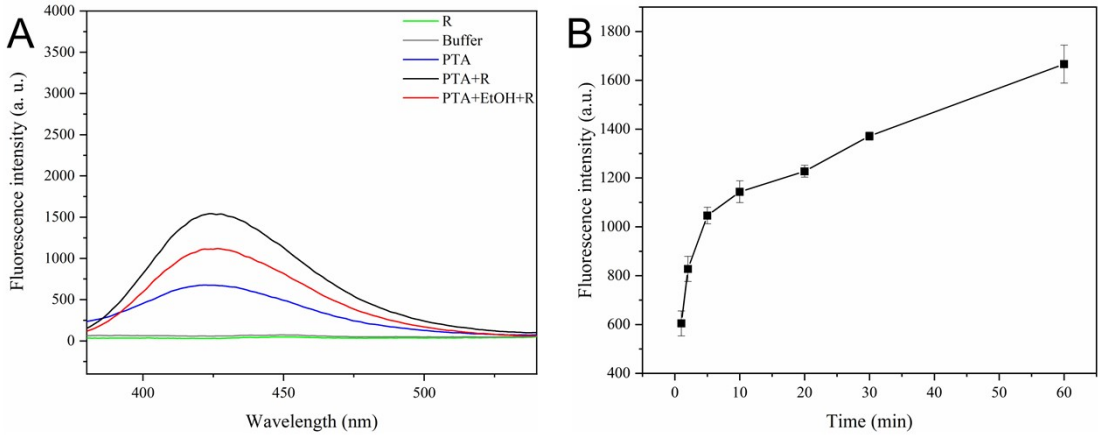

Figure S17. Fluorescence probe. (A) Fluorescence spectra with PTA probe. Ex, 312 nm. Reaction conditions: [tyrosine] = 1 mM, [PTA] = 1 mM, [ascorbic acid] = 1 mM, [H_2O_2] = 2 mM, [nanozyme] = 0.4 mg mL^{-1}, initial pH = 4.5, temperature = 25 °C, reaction time = 1 h. (B) Evolution of fluorescence intensity of the PTA probe reaction with ·OH.

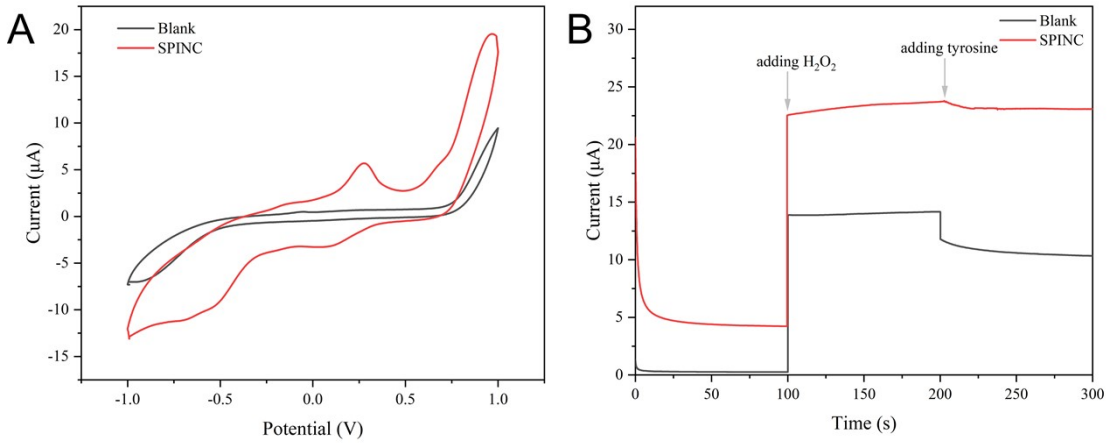

Figure S18. Electrochemical analysis. (A) Cyclic voltammograms response of tyrosine on bare and SPINC-modified glass carbon electrode. [tyrosine]=1 mM. (B) *i-t* curves. 1 V *vs*. saturated calomel electrode using 0.2 M glycine hydrochloride buffer as electrolyte. [H_2O_2]=50 mM, [tyrosine]=0.4 mM.

5. References**Uncategorized References**

1. J. Wang, RenliangQi, WeiSu, RongxinBinks, Bernard P.He, Zhimin, *Appl. Catal. B-Environ.* 2019,**254**.
2. J. Bing, D. Demin, G. Lizeng, Z. Mengjie, F. Kelong, T. Yan, X. Juqun, B. Yuhai, T. Zhou and G.G. Fu, *Nat. Protoc.* 2018.
3. B. Xu, H. Wang, W. Wang, L. Gao, S. Li, X. Pan, H. Wang, H. Yang, X. Meng, Q. Wu, L. Zheng, S. Chen, X. Shi, K. Fan, X. Yan and H. Liu, *Angew. Chem. Int. Ed.* 2019,**58**, 4911-4916.
4. M.S. Kim, J. Lee, H.S. Kim, A. Cho, K.H. Shim, T.N. Le, S.S.A. An, J.W. Han, M.I. Kim and J. Lee, *Adv. Funct. Mater.* 2020,**30**, -.
5. X. Niu, QiurongZhu, WenleiLiu, DongTian, HangyuFu, ShaofangCheng, NanLi, SuiqiongSmith, Jordan N.Du, DanLin, Yuehe, *Biosens. Bioelectron.* 2019,**142**.
6. N. Cheng, J.C. Li, D. Liu, Y. Lin and D. Du, *Small*. 2019,**15**.
7. Jiao, Weiqing, Hongye, Chunrong, Yuehe and Chengzhou, *Anal. Chem.* 2019,**91**, 11994-11999.
8. W. Wu, L. Huang, E. Wang and S. Dong, *Chem. Sci.* 2020,**11**, 9741-9756.
9. S.C. Daubner, J. Melendez and P.F. Fitzpatrick, *Biochemistry*. 2000,**39**, 9652-9661.